

# Dislocation contrast in cathodoluminescence and electron-beam induced current maps on GaN(0001)

Karl K. Sabelfeld

*Institute of Computational Mathematics and Mathematical Geophysics,  
Russian Academy of Sciences and Novosibirsk State University, Lavrentiev Prosp. 6, 630090 Novosibirsk, Russia.*

Vladimir M. Kaganer, Carsten Pfüller, and Oliver Brandt

*Paul-Drude-Institut für Festkörperelektronik, Hausvogteiplatz 5–7, 10117 Berlin, Germany*

(Dated: November 14, 2018)

We theoretically analyze the contrast observed at the outcrop of a threading dislocation at the GaN(0001) surface in cathodoluminescence and electron-beam induced current maps. We consider exciton diffusion and recombination including finite recombination velocities both at the planar surface and at the dislocation. Formulating the reciprocity theorem for this general case enables us to provide a rigorous analytical solution of this diffusion-recombination problem. The results of the calculations are applied to an experimental example to determine both the exciton diffusion length and the recombination strength of threading dislocations in a free-standing GaN layer with a dislocation density of  $6 \times 10^5 \text{ cm}^{-2}$ .

## I. INTRODUCTION

Early GaN-based light emitting diodes exhibited an external quantum efficiency of 4% despite containing threading dislocations with a density exceeding  $10^{10} \text{ cm}^{-2}$  [1]. This fact was met with considerable surprise, since other III-V semiconductors require drastically lower dislocation densities for reaching comparable efficiencies. To explain this phenomenon, it was proposed that dislocations in group-III nitrides are more benign than in other III-V compounds due to their high ionicity [1]. Alternatively, it was suggested that the diffusion length of minority charge carriers in GaN is smaller than the average distance between dislocations [2]. In later work, however, it was often reported that the diffusion length seems to be actually limited by this distance [3–6].

In cathodoluminescence (CL) or electron-beam induced current (EBIC) maps of the surface of heteroepitaxial GaN(0001) layers, threading dislocations are observed as dark spots directly reflecting the fact that they represent nonradiative centers [2]. Intensity profiles recorded across these areas of reduced luminous efficiency contain, in principle, information on both the minority-carrier (or, in GaN, exciton) diffusion length and the recombination strength of the dislocation [7]. To determine these quantities, however, it is required to consider the generation, diffusion and recombination of electron-hole pairs in the presence of a surface and a dislocation both possessing finite recombination strengths. This problem belongs to the classical problems of semiconductor physics and is under investigation since the 1950s [8–11], but a general solution has not been obtained so far. In particular, most of the existing theoretical work [7, 12–17] is restricted to either zero or infinite surface recombination velocity in addition to an infinite recombination strength at the dislocation, with the sole exception of the study by Jakubowicz [15] in which a finite recombination strength was introduced in an *ad hoc* fashion.

This body of theoretical understanding has been largely ignored by experimentalists. Rosner *et al.* [2] were the first to correlate the outcrops of dislocations visible in atomic force

micrographs of a GaN(0001) layer with the contrast fluctuations in CL maps. Due to the high dislocation density in the layer under investigation, individual dislocations were not resolved in the CL map, and the authors hence resorted to a simple phenomenological expression (first proposed by Suzuki and Matsumoto [18]) for describing the impact of dislocations on the CL intensity. In subsequent experimental work, individual dislocations were resolved in CL maps which would have been eligible objects for a more detailed analysis using appropriate models. However, in all of these studies [2, 3, 5, 19–23], the simple expression proposed by Rosner *et al.* [2] was adopted despite the fact that it does not represent a sensible approximation of the intensity profile across threading dislocations even in the most simple case of zero surface recombination velocity and infinite recombination strength at the dislocations.

This fact has recently been noted by Yakimov [24], who pointed out that the analysis of the experimental data in this purely empirical way leads to a significant underestimation of the exciton diffusion length. As a consequence, values for the exciton diffusion length derived in this way from CL or EBIC maps are to be viewed with caution [25]. Since either of these techniques gives, in principle, simultaneous access to three technologically important quantities (the exciton diffusion length, the surface recombination velocity, and the dislocation recombination strength), the problem clearly merits further theoretical and experimental attention.

In the present paper, we derive a rigorous analytical solution for the problem of excitons being generated within a finite volume and subsequently diffusing and recombining in the bulk as well as annihilating at the surface and at threading dislocations with arbitrary recombination velocities. For this purpose, the reciprocity theorem [14] is generalized. The solution of the problem for finite exciton recombination velocities at the planar surface is obtained by considering, instead of the half-space, a finite-thickness slab, whose thickness can be taken sufficiently large. This solution is also generalized for the case of thin films with finite recombination velocity at the back surface, as it is required for solar cells [26, 27]. The

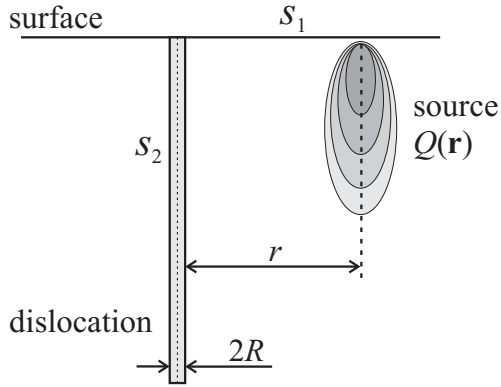


FIG. 1. Schematic depiction of a CL or EBIC experiment in the close vicinity of a surface and a dislocation. The incident electron beam creates a spatial distribution  $Q(\mathbf{r})$  of excitons, which then diffuse with a diffusivity  $D$  and recombine with an effective lifetime  $\tau$  in a semi-infinite layer with a surface having a surface recombination velocity  $S_1$  intersected by a threading dislocation with a recombination velocity  $S_2$ .

solution for a point source of excitons (the Green function) is directly convolved with the numerically calculated distributions of excitons generated by electron beams of different energies. The results of the calculations are applied to describe the contrast of threading dislocations in a freestanding GaN layer with an average distance between dislocations of more than  $10\ \mu\text{m}$ . A fit of the expression derived in this work to an experimental profile yields both the exciton diffusion length and the recombination strength at the dislocation.

## II. GENERAL EQUATIONS

We consider the generation of electron-hole pairs by an electron beam incident on the surface of a GaN{0001} layer with the three-dimensional generation function  $Q(\mathbf{r})$ . Because of the exciton binding energy of 26 meV in GaN, these electron-hole pairs rapidly bind to form excitons which then diffuse as a stable entity up to room temperature. Our aim is to solve the exciton diffusion-recombination problem in the half-space containing a dislocation line normal to the surface, as shown in Fig. 1. After forming from the high energy electron-hole cloud generated by the incident electron beam, these excitons will diffuse, recombine in the bulk, or annihilate non-radiatively at both the free surface of the half-space and the dislocation.

The diffusion and recombination of excitons generated by the source  $Q(\mathbf{r})$  are described by the three-dimensional diffusion-recombination equation

$$D\Delta n(\mathbf{r}) - n(\mathbf{r})/\tau + Q(\mathbf{r}) = 0, \quad (1)$$

where  $D$  is the diffusion coefficient and  $\tau$  the lifetime of excitons, describing their recombination in the bulk. This latter quantity includes both radiative and nonradiative contributions, i. e.,  $1/\tau = 1/\tau_r + 1/\tau_{nr}$ .

Nonradiative exciton annihilation at the surfaces is described by the boundary conditions

$$D \frac{\partial n(\mathbf{r})}{\partial v_k} + S_k n(\mathbf{r}) = 0, \quad \mathbf{r} \in \Gamma_k, \quad (2)$$

where  $\Gamma_k$  are the surfaces,  $v_k$  the surface normals,  $S_k$  the surface recombination velocities, and  $k = 1, 2$  correspond to the planar surface of the half-space and the cylindrical surface of the dislocation, respectively.

The total number of excitons annihilating at the respective surfaces is equal to the fluxes integrated over these surfaces,

$$I_k = D \int_{\Gamma_k} \frac{\partial n(\mathbf{r})}{\partial v_k} d\sigma_k. \quad (3)$$

Particularly, the flux of excitons to the planar surface  $I_1$  can be measured in an EBIC experiment, using a Schottky barrier to dissociate excitons into electrons and holes and separating them prior to recombination. The CL intensity is proportional to the total number of excitons recombining radiatively in the bulk. This quantity can be calculated by subtracting the fluxes to the surfaces  $I_1$  and  $I_2$  from the total number of excitons produced by the source,  $I_0 = \int Q(\mathbf{r}) dV$ , so that  $I_{\text{CL}} = \eta(I_0 - I_1 - I_2)$ , where  $\eta = \tau/\tau_r$  is the internal quantum efficiency, i. e., the fraction of excitons recombining radiatively. Since the measured CL intensity is arbitrarily scaled, the factor  $\eta$  can be included in the normalization constant and is omitted in the further analysis. Thus, our purpose is to calculate the fluxes to the surfaces  $I_1$  and  $I_2$ .

It is convenient to multiply Eqs. (1)–(3) with  $\tau$  and to introduce the diffusion length  $\Lambda = (D\tau)^{1/2}$  and the surface recombination lengths  $l_k = S_k\tau$ . The length  $l_1$  describes recombination at the planar surface, while the length  $l_2$  is the corresponding quantity at the dislocation. Then, all parameters entering the problem are quantities with the dimension of lengths: in addition to the three lengths  $\Lambda, l_1, l_2$ , we need to consider the radius  $R$  of the dislocation. Since Eqs. (1)–(3) are linear, it is sufficient to consider a point source of excitons in an arbitrary point  $\mathbf{r}'$ ,  $Q(\mathbf{r}) = \delta(\mathbf{r} - \mathbf{r}')$ , and calculate the Green function  $G(\mathbf{r}, \mathbf{r}')$ . Then, the solution for any finite source  $Q(\mathbf{r})$  can be obtained as a convolution

$$I(\mathbf{r}) = \int G(\mathbf{r}, \mathbf{r}') Q(\mathbf{r}') d\mathbf{r}'. \quad (4)$$

Hence, the problem can be finally formulated as follows. The distribution of excitons is governed by the three-dimensional diffusion-annihilation equation

$$\Lambda^2 \Delta G(\mathbf{r}, \mathbf{r}') - G(\mathbf{r}, \mathbf{r}') + \delta(\mathbf{r} - \mathbf{r}') = 0, \quad (5)$$

with third-type boundary conditions (Robin boundary conditions) at the planar surface of half-space ( $k = 1$ ) and at the cylindrical surface of the dislocation ( $k = 2$ )

$$\Lambda^2 \frac{\partial G(\mathbf{r}, \mathbf{r}')}{\partial v_k} + l_k G(\mathbf{r}, \mathbf{r}') = 0, \quad \mathbf{r} \in \Gamma_k. \quad (6)$$

The boundary condition at large distances from the source and the dislocation is  $G(\mathbf{r}, \mathbf{r}') \rightarrow 0$  at  $\mathbf{r} \rightarrow \infty$ . Our aim is to calculate the total fluxes to each surface,

$$I_k(\mathbf{r}') = \int_{\Gamma_k} \frac{\partial G(\mathbf{r}, \mathbf{r}')}{\partial v_k} d\sigma_k. \quad (7)$$

### III. THE RECIPROCITY THEOREM

The reciprocity theorem was formulated and proven by Donolato [14] for the case when the planar surface is a perfect sink (infinite surface recombination velocity): in this case, the local generation of excitons with integral detection of their recombination is equivalent to their uniform generation with local detection. Here, we extend this theorem to arbitrary finite surface recombination velocities.

Let us show that the integral  $I_i(\mathbf{r})$  given by Eq. (7) is identically equal to  $\Lambda^2 F(\mathbf{r})$ , where  $F(\mathbf{r})$  is the solution of the following homogeneous boundary value problem:

$$\Lambda^2 \Delta F(\mathbf{r}) - F(\mathbf{r}) = 0, \quad (8)$$

with the boundary condition at the  $i$ th surface modified as follows:

$$\Lambda^2 \frac{\partial F(\mathbf{r})}{\partial \mathbf{v}_i} + l_i [F(\mathbf{r}) - 1] = 0, \quad \mathbf{r} \in \Gamma_i, \quad (9)$$

while on all other surfaces ( $k \neq i$ ) the boundary condition remains unchanged,

$$\Lambda^2 \frac{\partial F(\mathbf{r})}{\partial \mathbf{v}_k} + l_k F(\mathbf{r}) = 0, \quad \mathbf{r} \in \Gamma_k, \quad k \neq i. \quad (10)$$

The proof is based on Green's formula

$$\int (F \Delta G - G \Delta F) dV = \sum_k \int_{\Gamma_k} \left( F \frac{\partial G}{\partial \mathbf{v}_k} - G \frac{\partial F}{\partial \mathbf{v}_k} \right) d\sigma_k, \quad (11)$$

where the integral in the left-hand side is over the volume and the integral in the right-hand side is a sum of integrals over all surfaces bounding this volume. A substitution of Eqs. (5) and (8) reduces Green's formula to

$$\frac{F(\mathbf{r}')}{\Lambda^2} = - \sum_k \int_{\Gamma_k} \left( F(\mathbf{r}) \frac{\partial G(\mathbf{r}, \mathbf{r}')}{\partial \mathbf{v}_k} - G(\mathbf{r}, \mathbf{r}') \frac{\partial F(\mathbf{r})}{\partial \mathbf{v}_k} \right) d\sigma_k. \quad (12)$$

All surface integrals with  $k \neq i$  vanish since the functions  $F$  and  $G$  satisfy the same boundary conditions, (6) and (10), at these surfaces. The integral over the remaining boundary  $\Gamma_i$  coincides with the right-hand side of Eq. (7), which completes the proof.

### IV. CALCULATION OF THE FLUXES

Before considering the most general case of finite recombination velocities on both surfaces, the planar surface of the half-space and the cylindrical surface of the dislocation, we analyze two limiting cases. In the first case, we assume that excitons do not annihilate at the planar surface ( $l_1 \rightarrow 0$ ). An exciton diffusing to the surface is thus "reflected" by it and continues its diffusional motion in the half-space. The continuation of its random trajectory is a mirror reflection of the trajectory that it would have in an infinite space with an infinitely long dislocation. Thus, in this case the solution of the

diffusion problem in the half-space is the same as in the infinite space.

The second case is the one considered by Donolato [17]: the planar surface is a perfect sink for excitons ( $l_1 \rightarrow \infty$ ). In this case we calculate, in addition to the total flux of excitons to the planar surface, the total flux to the dislocation. The former quantity (calculated by Donolato) gives the EBIC intensity (requiring a Schottky barrier or a  $p$ - $n$  junction to dissociate the excitons), while the latter is needed to obtain the CL intensity.

#### A. Reflection (Neumann) boundary condition at the planar surface

In this case ( $l_1 \rightarrow 0$ ) there is no flux at the planar surface, and we need to calculate the flux to the cylindrical surface of the dislocation. From the reciprocity theorem, this flux  $f(r, z)$  (where  $r, z$  are cylindrical coordinates of the point source of excitons) is a solution of the equation

$$\Delta_r f(r, z) + \frac{\partial^2 f(r, z)}{\partial z^2} - \Lambda^{-2} f(r, z) = 0 \quad (13)$$

with the boundary conditions

$$\left. \frac{\partial f}{\partial z} \right|_{z=0} = 0, \quad \left( -\Lambda^2 \frac{\partial f}{\partial r} + l_2 f \right) \Big|_{r=R} = l_2. \quad (14)$$

The derivative  $\partial f / \partial r$  enters the second boundary condition (14)<sub>2</sub> with negative sign, since the outer normal  $\mathbf{v}_2$  in Eqs. (11) and (12) is along the negative direction of  $r$ .

Since the reflecting planar boundary can be replaced by continuation of the medium to the other half-space, we seek for a solution that does not depend on  $z$ . Equation (13) and the first boundary condition (14)<sub>1</sub> are satisfied with  $f(r, z) = CK_0(r/\Lambda)$ , where  $K_0(x)$  is the zero order modified Bessel function of the second kind. The coefficient  $C$  is determined from the second boundary condition (14)<sub>2</sub>. The solution is

$$f(r) = \frac{l_2 K_0(r/\Lambda)}{\Lambda K_1(R/\Lambda) + l_2 K_0(R/\Lambda)}, \quad (15)$$

where  $K_1(x)$  is the first order modified Bessel function of the second kind.

For the discussion below in Sec. IV C, it is instructive to present also a more formal, albeit more lengthy, derivation of Eq. (15). A solution of Eq. (13) can be sought in the form

$$f(r, z) = \int_0^\infty C(q) K_0(\mu_q r) \cos(qz) dq, \quad (16)$$

where

$$\mu_q = \sqrt{q^2 + \Lambda^{-2}}. \quad (17)$$

The term  $\cos(qz)$  in the integral provides the first boundary condition (14)<sub>1</sub>. The second boundary condition (14)<sub>2</sub> can be

written as

$$\int_0^{\infty} C(q) [\Lambda K_1(R/\Lambda) + l_2 K_0(R/\Lambda)] \cos(qz) dq = l_2. \quad (18)$$

For the right-hand side of this equation, we use the identity

$$1 = 2 \int_0^{\infty} \delta(z) \cos(qz) dz, \quad (19)$$

where  $\delta(x)$  is the Dirac delta function, and thus obtain

$$C(q) = \frac{2l_2 \delta(q)}{\Lambda K_1(R/\Lambda) + l_2 K_0(R/\Lambda)}. \quad (20)$$

Substituting this expression into Eq. (16), we arrive at the same result (15).

## B. Absorption (Dirichlet) boundary condition at the planar surface

### 1. Flux to the dislocation

We now consider the planar boundary as a perfect sink for excitons with surface recombination velocity  $l_1 \rightarrow \infty$ , and calculate first the flux  $f(x, z)$  of the excitons produced by a point source at  $(r, z)$  to the cylinder  $r = R$ . The reciprocity theorem provides for the function  $f(r, z)$  the boundary value problem

$$\Delta_r f(r, z) + \frac{\partial^2 f(r, z)}{\partial z^2} - \Lambda^{-2} f(r, z) = 0, \quad (21)$$

$$f|_{z=0} = 0, \quad \left( -\Lambda^2 \frac{\partial f}{\partial r} + l_2 f \right) \Big|_{r=R} = l_2. \quad (22)$$

We seek the solution in the form

$$f(r, z) = \int_0^{\infty} C(q) K_0(\mu_q r) \sin(qz) dq \quad (23)$$

and represent the boundary condition at the cylinder surface (22)<sub>2</sub> as

$$\int_0^{\infty} C(q) [l_2 K_0(\mu_q R) + \Lambda^2 \mu_q K_1(\mu_q R)] \sin(qz) dq = l_2. \quad (24)$$

Using in the right-hand side of this equation the equality

$$1 = \frac{2}{\pi} \int_0^{\infty} \frac{\sin(qz)}{q} dq, \quad (25)$$

we obtain the flux to the dislocation

$$f(r, z) = \frac{2}{\pi} \int_0^{\infty} \frac{l_2 K_0(\mu_q r) \sin(qz) dq}{q [l_2 K_0(\mu_q R) + \Lambda^2 \mu_q K_1(\mu_q R)]}. \quad (26)$$

### 2. Flux to the planar boundary

Let us calculate now the total flux  $g(r, z)$  to the planar surface of the excitons produced by a point source at  $(x, z)$ . According to the reciprocity theorem in Sec. III, the function  $g(r, z)$  satisfies the equation

$$\Delta_r g(r, z) + \frac{\partial^2 g(r, z)}{\partial z^2} - \Lambda^{-2} g(r, z) = 0 \quad (27)$$

and the boundary conditions

$$g|_{z=0} = 1, \quad \left( -\Lambda^2 \frac{\partial g}{\partial r} + l_2 g \right) \Big|_{r=R} = 0. \quad (28)$$

Let us find a function  $v(z)$  satisfying Eq. (27) and the first boundary condition (28)<sub>1</sub>, i.e.,

$$d^2 v/dz^2 - \Lambda^{-2} v = 0, \quad v(0) = 1. \quad (29)$$

The solution is  $v(z) = \exp(-z/\Lambda)$ . Let us introduce a new function  $u(r, z)$  by  $g(r, z) = v(z) - u(r, z)$ . Then, the boundary value problem can be written as

$$\Delta_r u(r, z) + \frac{\partial^2 u(r, z)}{\partial z^2} - \Lambda^{-2} u(r, z) = 0, \quad (30)$$

$$u|_{z=0} = 0, \quad \left( -\Lambda^2 \frac{\partial u}{\partial r} + l_2 u \right) \Big|_{r=R} = l_2 \exp(-z/\Lambda). \quad (31)$$

We seek for a solution in the form

$$u(r, z) = \int_0^{\infty} C(q) K_0(\mu_q r) \sin(qz) dq. \quad (32)$$

Equation (30) and the first boundary condition (31)<sub>1</sub> are satisfied, and the boundary condition (31)<sub>2</sub> at the surface of the cylinder  $r = R$  reads

$$\int_0^{\infty} C(q) [l_2 K_0(\mu_q R) + \Lambda^2 \mu_q K_1(\mu_q R)] \sin(qz) dq = l_2 \exp(-z/\Lambda). \quad (33)$$

The right-hand side of this equation can be represented as

$$l_2 \exp(-z/\Lambda) = \frac{2}{\pi} l_2 \int_0^{\infty} \frac{q \sin(qz)}{q^2 + \Lambda^{-2}} dq, \quad (34)$$

which gives  $C(q)$  and finally the flux to the planar surface

$$g(r, z) = \exp(-z/\Lambda) - \frac{2}{\pi} \int_0^{\infty} \frac{q l_2}{q^2 + \Lambda^{-2}} \frac{K_0(\mu_q r) \sin(qz) dq}{l_2 K_0(\mu_q R) + \Lambda^2 \mu_q K_1(\mu_q R)}. \quad (35)$$

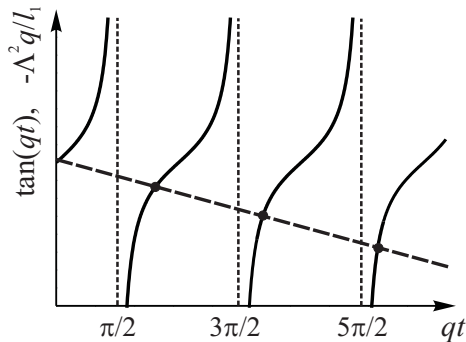


FIG. 2. Graphical representation of the eigenvalues  $q_n$  of Eq. (41).

### C. Finite recombination velocity at the planar surface (Robin boundary condition)

We have considered above two limiting cases, the absence of recombination at the planar surface ( $l_1 \rightarrow 0$ ) and the total annihilation of excitons at this boundary ( $l_1 \rightarrow \infty$ ). In this section, our aim is to generalize these results to the case of an arbitrary surface recombination velocity (an arbitrary  $l_1$ ). For this purpose, we consider, instead of the half-space, a slab with a finite thickness  $t$ , with the dislocation running across it. The solution is represented by series, rather than integrals. Taking  $t$  sufficiently large, we arrive at the solution for the half-space. First, we assume the absence of surface recombination at the back surface  $z = t$ . Second, we allow for an arbitrary surface recombination velocity also at the back surface to obtain a solution for thin films applicable, in particular, to the case of solar cells [26, 27].

#### 1. Flux to the dislocation

The reciprocity theorem states that the total flux  $f(r, z)$  to the surface of the cylinder from a point source at  $(x, z)$  is a solution of the diffusion equation

$$\Delta_r f(r, z) + \frac{\partial^2 f(r, z)}{\partial z^2} - \Lambda^{-2} f(r, z) = 0 \quad (36)$$

with the boundary conditions

$$\left( -\Lambda^2 \frac{\partial f}{\partial z} + l_1 f \right) \Big|_{z=0} = 0, \quad \left( -\Lambda^2 \frac{\partial f}{\partial r} + l_2 f \right) \Big|_{r=R} = l_2, \quad f(r, t) = 0. \quad (37)$$

The problem is solved by separation of vertical and radial variables. We first seek for eigenfunctions  $y_n(z)$  and eigenvalues  $q_n$  ( $n = 1, 2, \dots$ ) which are solutions of the ordinary differential equation

$$\frac{d^2 y_n}{dz^2} + q_n^2 y_n = 0 \quad (38)$$

with the boundary conditions

$$-\Lambda^2 \frac{dy_n}{dz} \Big|_{z=0} + l_1 y_n(0) = 0, \quad y_n(t) = 0. \quad (39)$$

The solutions of Eq. (38) satisfying the second boundary condition (39)<sub>2</sub> are

$$y_n(z) = p_n \sin[q_n(t - z)], \quad (40)$$

where the coefficients  $p_n$  will be chosen later. The first boundary condition (40)<sub>1</sub> gives rise to the equation

$$\tan(q_n t) = -\Lambda^2 q_n / l_1. \quad (41)$$

This equation has an infinite number of solutions  $q_n > 0$ ,  $n = 1, 2, \dots$ , as illustrated in Fig. 2. These solutions are the eigenvalues of the problem. Evidently, the  $n$ th root is restricted by  $n\pi/2 < q_n t < \pi + n\pi/2$ , so that all roots can easily be determined numerically.

The limiting cases considered in the two previous sections can be obtained from Eq. (41). The reflection boundary condition at the planar surface  $l_1 \rightarrow 0$  gives  $q_n t = (2n - 1)\pi/2$ , and the eigenfunctions (40) are  $y_n = p_n \cos(q_n z)$ , as also seen in Eq. (16). In the opposite limit of the absorption boundary condition,  $l_1 \rightarrow \infty$ , the eigenvalues are  $q_n t = n\pi$ , and the eigenfunctions  $y_n = p_n \sin(q_n z)$ , as in Eqs. (23) and (32).

The functions  $y_n(z)$  are orthogonal on  $[0, t]$ , and we choose the coefficients  $p_n$  in Eq. (40) by requiring the functions to be normalized:

$$\int_0^t y_n(z) y_{n'}(z) dz = \delta_{nn'}. \quad (42)$$

Making use of Eqs. (40) and (41), we find

$$p_n^2 = 2 \left[ t + \frac{l_1}{(l_1/\Lambda)^2 + (\Lambda q_n)^2} \right]^{-1}. \quad (43)$$

Now we seek the solution in the form

$$f(r, z) = \sum_{n=1}^{\infty} C_n y_n(z) K_0(\mu_n r), \quad (44)$$

with

$$\mu_n = \sqrt{q_n^2 + \Lambda^{-2}}, \quad (45)$$

thus generalizing Eqs. (16) and (17) to the case of a finite slab thickness.

The boundary condition at the cylinder surface (37)<sub>2</sub> reads

$$\sum_{n=1}^{\infty} C_n y_n(z) [l_2 K_0(\mu_n R) + \Lambda^2 \mu_n K_1(\mu_n R)] = l_2. \quad (46)$$

Multiplying this equation with  $y_n(z)$  and integrating over  $z$ , we find

$$C_n = \frac{l_2 p_n}{q_n} \frac{1 - \cos(q_n t)}{l_2 K_0(\mu_n R) + \Lambda^2 \mu_n K_1(\mu_n R)}. \quad (47)$$

Thus, the total flux  $f(r, z)$  of excitons to the dislocation from a point source at  $(r, z)$  is given by Eq. (44), where the eigenvalues  $q_n$  are solutions of Eq. (41), the functions  $y_n(z)$  are given by Eq. (40) and the coefficients  $C_n$  by Eq. (47).

## 2. Flux to the planar boundary

The flux to the planar surface  $g(r, z)$  due to a point source at  $(r, z)$  is given, by virtue of the reciprocity theorem, by a solution of the equation

$$\Delta_r g(r, z) + \frac{\partial^2 g(r, z)}{\partial z^2} - \Lambda^{-2} g(r, z) = 0 \quad (48)$$

with the boundary conditions

$$\left( -\Lambda^2 \frac{\partial g}{\partial z} + l_1 g \right) \Big|_{z=0} = l_1, \quad \left( -\Lambda^2 \frac{\partial g}{\partial r} + l_2 g \right) \Big|_{r=R} = 0, \\ g(r, t) = 0. \quad (49)$$

Similarly to Sec. IV B 2, we seek first for a function  $v(z)$  solving Eq. (48) with the boundary conditions (49) at  $z = 0$  and  $z = t$ , i. e.,

$$\frac{d^2 v}{dz^2} - \Lambda^{-2} v = 0, \quad \left( -\Lambda^2 \frac{dv}{dz} + l_1 v \right) \Big|_{z=0} = l_1, \quad v(t) = 0. \quad (50)$$

The solution is

$$v(z) = \frac{l_1 \sinh[(t-z)/\Lambda]}{\Lambda \cosh(t/\Lambda) + l_1 \sinh(t/\Lambda)}. \quad (51)$$

Now we introduce a new function  $u(r, z)$  with

$$g(r, z) = v(z) - u(r, z). \quad (52)$$

The boundary value problem for the function  $u(r, z)$  reads

$$\Delta_r u(r, z) + \frac{\partial^2 u(r, z)}{\partial z^2} - \Lambda^{-2} u(r, z) = 0, \quad (53)$$

$$\left( -\Lambda^2 \frac{\partial u}{\partial z} + l_1 u \right) \Big|_{z=0} = 0, \\ \left( -\Lambda^2 \frac{\partial u}{\partial r} + l_2 u \right) \Big|_{r=R} = l_2 v(z), \quad u(r, t) = 0. \quad (54)$$

We seek a solution in the same form as in Eq. (44) above,

$$u(r, z) = \sum_{n=1}^{\infty} C_n y_n(z) K_0(\mu_n r), \quad (55)$$

and arrive at the equations for the coefficients  $C_n$ :

$$\sum_{n=1}^{\infty} C_n y_n(z) [l_2 K_0(\mu_n R) + \Lambda^2 \mu_n K_1(\mu_n R)] = l_2 v(z), \quad (56)$$

that replace Eq. (46) in the previous section. Multiplying this equation by  $y_n(z)$  and taking into account that the functions  $y_n(z)$  are orthogonal and normalized according to Eq. (42), we find the coefficients

$$C_n = \frac{l_1 l_2 \Lambda p_n}{\Lambda \cosh(t/\Lambda) + l_1 \sinh(t/\Lambda)} \\ \times \frac{\cosh(t/\Lambda) \sin(q_n t) - q_n \Lambda \sinh(t/\Lambda) \cos(q_n t)}{(1 + q_n^2 \Lambda^2) [l_2 K_0(\mu_n R) + \Lambda^2 \mu_n K_1(\mu_n R)]}. \quad (57)$$

Thus, the total flux  $g(r, z)$  to the planar surface from a point source at  $(r, z)$  is given by Eq. (52), where  $v(z)$  is defined by Eq. (51) and  $u(r, z)$  by Eq. (55), with the coefficients  $C_n$  given by Eq. (57). The function  $g(r, z)$  directly gives the EBIC signal, while the CL intensity is equal to  $1 - [f(r, z) + g(r, z)]$ , where the function  $f(r, z)$  is given by Eq. (44).

## 3. Finite recombination velocity at the back surface

A finite exciton recombination velocity  $S_3$  at the back surface  $z = t$  gives rise to a surface recombination length  $l_3 = S_3 \tau$ , analogously to the recombination length  $l_1$  at the planar surface  $z = 0$  and the recombination length  $l_2$  at the dislocation  $r = R$ . Then, the boundary condition (37)<sub>3</sub> for the diffusion equation (36) is replaced with

$$\left( \Lambda^2 \frac{\partial f}{\partial z} + l_3 f \right) \Big|_{z=t} = 0, \quad (58)$$

and the boundary condition (39)<sub>2</sub> for the eigenfunctions  $y_n(z)$  becomes

$$\Lambda^2 \frac{dy_n}{dz} \Big|_{z=t} + l_3 y_n(t) = 0. \quad (59)$$

The solutions of Eq. (38) with boundary conditions (39)<sub>1</sub> and (59) are

$$y_n(z) = p_n [\sin(q_n z) + (\Lambda^2 q_n / l_1) \cos(q_n z)], \quad (60)$$

where the eigenvalues  $q_n$  are the solutions of the equation

$$\tan(q_n t) = \frac{(l_1 + l_3) q_n}{\Lambda^2 q_n^2 - l_1 l_3 / \Lambda^2} \quad (61)$$

and the coefficients  $p_n$  providing the normalization condition (42) are given by

$$p_n^2 = \left\{ \frac{l_1^2 + q_n^2 \Lambda^4}{2 l_1^2} \left[ t + \frac{\Lambda^2 (l_1 + l_3) (l_1 l_3 + q_n^2 \Lambda^4)}{(l_1^2 + q_n^2 \Lambda^4) (l_3^2 + q_n^2 \Lambda^4)} \right] \right\}^{-1}. \quad (62)$$

The functions  $y_n(z)$  defined by Eq. (60) can be used in Eqs. (44) and (55) to obtain the fluxes to the dislocation and to the upper planar boundary, respectively.

## V. EXAMPLES

### A. CL profile in the absence of surface recombination

Let us analyze first the most simple case for which the recombination of excitons at the planar surface is absent. The CL intensity is equal to  $I_{CL}(r) = 1 - f(r)$ , where  $f(r)$  is given by Eq. (15). Since the radius of the dislocation  $R$  is always small compared to the diffusion length  $\Lambda$ , we can use

the expansion of the Bessel function for small arguments,  $K_1(x) \approx 1/x$ , and represent the CL intensity as

$$I_{\text{CL}}(r) = 1 - \frac{K_0(r/\Lambda)}{K_0(R/\Lambda) + \Lambda^2/Rl_2}. \quad (63)$$

If the dislocation is a perfect sink for excitons,  $l_2 \rightarrow \infty$ , and Eq. (63) reduces to

$$I_{\text{CL}}(r) = 1 - \frac{K_0(r/\Lambda)}{K_0(R/\Lambda)}. \quad (64)$$

This expression was derived first by Brantley *et al.* [28] for spatially uniform generation of carriers and local detection, whereas we consider local (point source) generation and integral detection. At the first glance, this coincidence is surprising. However, it follows directly from the reciprocity theorem proven in Sec. III: the problems are actually exactly reciprocal, so their solutions coincide. In the absence of surface recombination, the diffusion problems in half-space and in infinite space also coincide, since the trajectory of the diffusional motion of an exciton reflected from the surface of the half-space is a mirror image of the continuation of that random trajectory in the other half-space. Hence, the solution of the point-generation problem in the half-space in the absence of surface recombination and with the dislocation as a perfect sink is given by Eq. (64). The generalization to the case of finite recombination velocities at the surface and at the dislocation is derived in Sec. IV.

Suzuki and Matsumoto [18] as well as Lax [29] noted that Eq. (64) may, for large arguments, be approximated by replacing the Bessel function by its asymptotic

$$I_{\text{CL}}(r) = 1 - \exp(-r/\Lambda). \quad (65)$$

This approximation was used in essentially all studies aiming to derive the exciton diffusion length in GaN from CL experiments [3, 19–23]. While it may be justified to use Eq. (64) in the case when surface recombination can be neglected, the replacement of the Bessel function by Eq. (65) is a valid approximation only at  $r \gg \Lambda$ , where the CL contrast vanishes. In fact, a reliable determination of the diffusion length requires the accurate description of the profile at  $r \lesssim \Lambda$ , which is not possible with Eq. (65).

Figure 3(a) compares the dislocation contrast given by Eq. (64) with its common replacement [2, 3, 19–23] by an exponential function [Eq. (65)] for the case when the dislocation acts as a perfect sink for excitons. The exciton diffusion length is assumed to be  $\Lambda = 0.5 \mu\text{m}$ . The dislocation radius for the exciton diffusion problem cannot be determined from experiments, and we assume it to be of atomic scale,  $R = 1 \text{ nm}$ . Since the ratio  $R/\Lambda$  is certainly small and the Bessel function  $K_0(R/\Lambda)$  depends on its argument only logarithmically for small arguments, the choice of  $R$  does not play a role when the dislocation acts as a perfect sink for the excitons ( $l_2 \rightarrow \infty$ ). It is evident from Fig. 3(a) that the replacement of the solution (64) (thick line) with the exponential function (65) (dashed line), as it is done in Refs. [2, 3, 19–23], is an exceedingly poor approximation which leads to a large error in the determination of the exciton diffusion length from the CL contrast of dislocations.

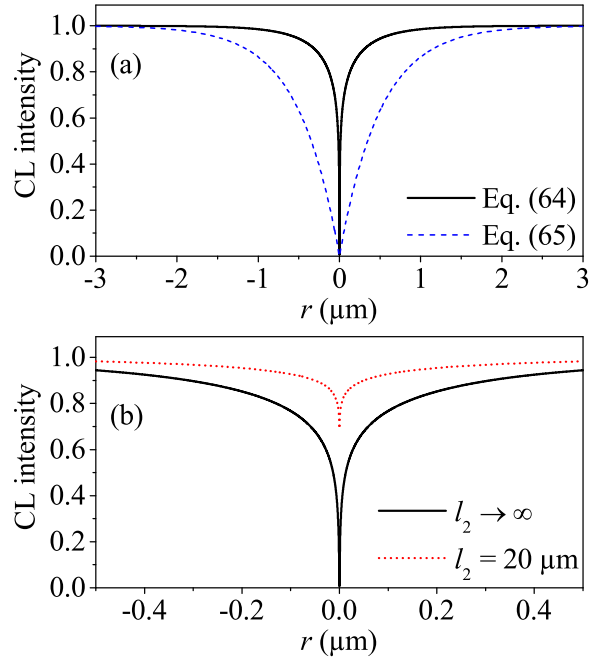


FIG. 3. Calculated CL contrast of a dislocation in the absence of surface recombination at the planar surface ( $l_1 = 0$ ). An exciton diffusion length of  $\Lambda = 0.5 \mu\text{m}$  and a dislocation radius of  $R = 1 \text{ nm}$  are assumed. (a) Infinite recombination velocity at the dislocation line ( $l_2 \rightarrow \infty$ ): Comparison of the exact solution Eq. (64) (solid line) and its exponential asymptotic approximation Eq. (65) (dashed line). (b) A comparison of infinite [ $l_2 \rightarrow \infty$ , Eq. (64), thick line] and finite [ $l_2 = 20 \mu\text{m}$ , Eq. (63), dotted line] recombination velocities at the dislocation.

Figure 3(b) shows the effect of a finite recombination velocity at the dislocation (finite  $l_2$ ). The CL intensity depends on the product  $l_2 R$ , as it follows from Eq. (63). Since both parameters characterizing a dislocation,  $R$  and  $l_2$ , are difficult to determine separately from an experiment, we keep a constant value of  $R = 1 \text{ nm}$  in the calculations below and vary  $l_2$  to match the contrast. The decrease of this product results in a decrease of the contrast, as it is shown by the dotted line in Fig. 3(b).

## B. The effect of surface recombination

Figure 4 presents the calculated dislocation contrast for a point source of excitons located at a distance  $r$  from the dislocation line and at a depth  $z = 10 \text{ nm}$  from the surface. In these calculations, we assume that the dislocation line is a perfect sink for the excitons ( $l_2 \rightarrow \infty$ ). We use the formulas derived above to calculate the total exciton flux to the dislocation  $f$  and their total flux to the planar surface  $g$  (the EBIC signal in an appropriately designed experiment). The remaining quantity  $1 - (f + g)$  accounts for the fraction of excitons experiencing recombination in the bulk. As we have already discussed in Sec. II, only a fraction  $\eta = \tau/\tau_r$  of excitons recombines radiatively and thus contributes to the experimental observable, i. e., the CL intensity. However, since the CL intensity cannot

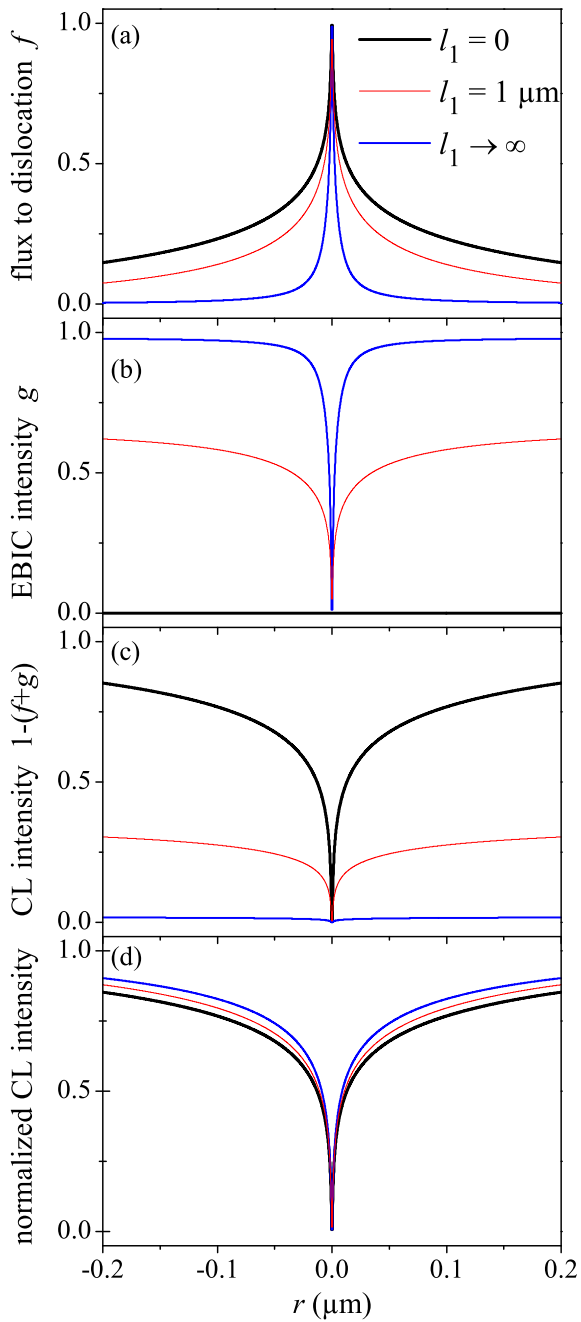


FIG. 4. (a) Total flux of excitons to the dislocation  $f$ , (b) total flux to the planar surface  $g$  (the EBIC signal), (c) fraction of excitons experiencing radiative recombination in the bulk  $1 - (f + g)$  (the CL intensity), and (d) CL intensity scaled by the intensity far from the dislocation. A point source of excitons is located at a distance  $r$  from the dislocation and at a depth  $z = 10$  nm from the surface. A diffusion length of  $\Lambda = 0.5$   $\mu\text{m}$  is assumed. The dislocation is considered to be a perfect sink for excitons ( $l_2 \rightarrow \infty$ ), and the surface recombination velocity is zero ( $l_1 = 0$ , black lines), finite ( $l_1 = 1$   $\mu\text{m}$ , red lines), or infinite ( $l_1 \rightarrow \infty$ , blue lines).

be measured on an absolute scale, this factor can be omitted in the analysis.

One can see from Fig. 4(a) that the exciton flux to the dislocation  $f$  is maximum when recombination at the planar surface is absent and minimum when the planar surface acts as a perfect sink for excitons reaching it. In turn, the flux to the planar surface in Fig. 4(b) is absent when the surface recombination is absent and maximum when the surface acts as a perfect absorber. In this latter case, as it is seen by the blue line in Fig. 4(c), the remaining fraction of excitons that are radiatively recombining in the bulk and actually contribute to the CL signal is small. Far from the dislocation line, only 2% of the excitons are recombining radiatively, since the source is close to the surface.

Since the CL intensities cannot be compared on the absolute scale, they need to be normalized by calculating the contrast  $(I - I_\infty)/I_\infty$ , where  $I_\infty$  is the intensity far from the dislocation. Then all CL curves tend to 1 in the limit  $r \rightarrow \infty$ . The result of this normalization is presented in Fig. 4(d), and it is seen that the normalized intensity only weakly depends on the surface recombination velocity. Note that the calculations in Fig. 4 are performed assuming that the dislocation line is a perfect sink for the excitons. If the dislocation possesses a finite recombination velocity (finite  $l_2$ ), the contrast decreases, in the same way as it is shown by the dotted line in Fig. 3(b).

### C. Finite source size

The solutions obtained in Sec. IV are the Green functions that describe the CL and EBIC signals due to a point source of

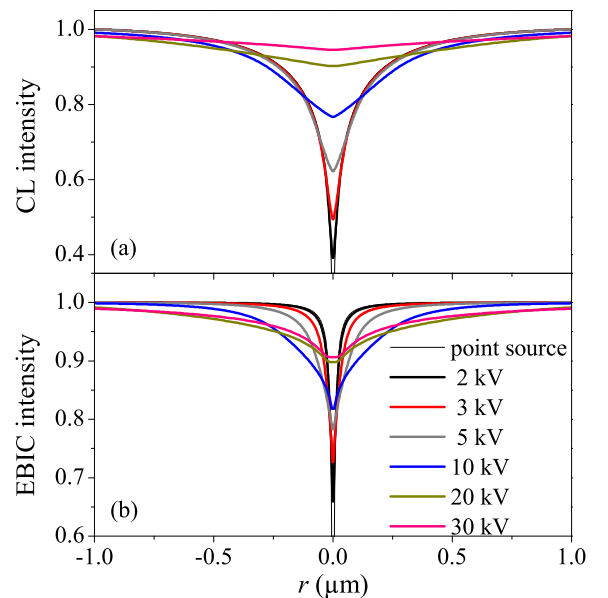


FIG. 5. Calculated (a) CL and (b) EBIC contrast of a dislocation for different acceleration voltages of the electron beam. For the calculations, we assumed total annihilation of excitons at both the planar surface and at the dislocation (i.e.,  $l_1 \rightarrow \infty$ ,  $l_2 \rightarrow \infty$ ) and an exciton diffusion length of  $\Lambda = 0.5$   $\mu\text{m}$ .

excitons located at a distance  $r$  from the dislocation line and at a depth  $z$ . Since the diffusion problem is linear, the solution for an arbitrary finite source of excitons can be obtained as the convolution integral (4) of the Green function with the initial exciton distribution produced by the electron beam.

We employ the common assumption [30] that the number of thermalized electron-hole pairs (and hence excitons) produced in a volume element by the electron beam is proportional to the energy loss of the electrons in that volume, and use the Monte Carlo software CASINO [31, 32] to simulate the distributions of the energy losses at different acceleration voltages of the electron beam. We do not attempt to describe the initial exciton distribution by any analytical function, as it is done in other works [19, 33–37]. Rather, we simulate the initial exciton distribution by CASINO on a  $100 \times 100 \times 100$  grid and perform a direct summation of intensities considering each point of the grid as a point source, with the number of excitons in it proportional to the local energy loss of the electron beam.

Figures 5(a) and 5(b) compare, respectively, the CL and EBIC profiles at different acceleration voltages, assuming that both the planar surface and the dislocation are perfect sinks for the excitons ( $l_1 \rightarrow \infty$ ,  $l_2 \rightarrow \infty$ ). One can see that, for low acceleration voltages up to 3 kV, the profiles are affected only in a very narrow range near the dislocation line. As the acceleration voltage is beyond 3 kV, however, the profiles broaden significantly and the contrast decreases. The CL profiles are noticeably broader than the EBIC profiles. The widths of the CL profiles monotonously increase with the acceleration voltage, while the EBIC profiles saturate at high acceleration voltages, since the excitons that are generated at depths exceeding the diffusion length do not reach the surface [38].

#### D. Experimental profiles

CL spectroscopy was carried out in a Zeiss Ultra55 field-emission scanning electron microscope equipped with a Gatan MonoCL4 system and a He-cooling stage. A photomultiplier tube was used for the acquisition of panchromatic CL images. The acceleration voltage was set to 3 kV, and the probe current of the electron beam to 0.75 nA, with the aim to minimize the generation volume of excitons as much as possible [cf. Fig. 5(a)].

Figure 6 presents a panchromatic CL map of a  $\approx 350 \mu\text{m}$  thick free-standing GaN(0001) layer grown by hydride vapor phase epitaxy. The average threading dislocation density present at the surface of this layer amounts to about  $6 \times 10^5 \text{ cm}^{-2}$ , low enough to allow us to perform intensity line scans of individual dislocations not influenced by other ones. Furthermore, the exciton diffusion length in this sample is certainly not limited by the average distance between dislocations.

Figure 7 compares an experimental intensity profile with the calculated one based on the analytical expressions derived in Sec. IV C and a summation over the initial spatial distribution of the excitons, simulated by the calculated energy loss distribution of the incident electron beam. As we have al-

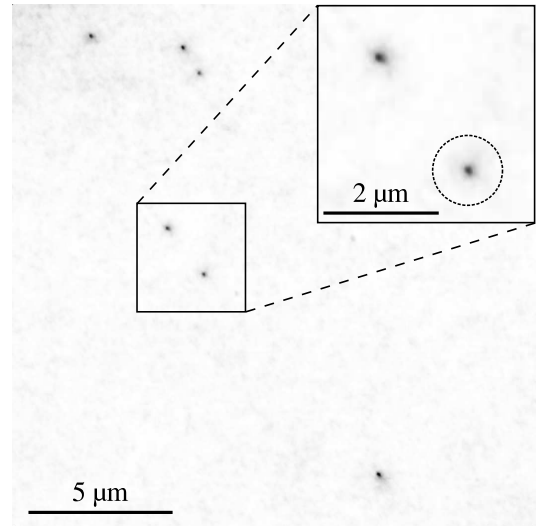


FIG. 6. Panchromatic CL map of the free-standing GaN(0001) layer under investigation over an area of  $330 \mu\text{m}^2$ . The CL intensity is essentially uniform except at the outcrops of threading dislocations, where clearly defined dark spots are observed. The inset shows a magnified view of two threading dislocations. For further analysis, a linescan was taken across the dislocation marked with a dashed circle (see Fig.7).

ready seen in Fig. 4(d), the CL intensity profile, after it is scaled such that the intensity far from the dislocation is unity, is fairly insensitive to the recombination velocity at the planar boundary. Hence, we estimate the surface recombination length using the results of an independent experimental determination of the surface recombination velocity and the exciton lifetime in GaN epilayers grown by metalorganic chemical-vapor deposition [39]. This latter study provides values of

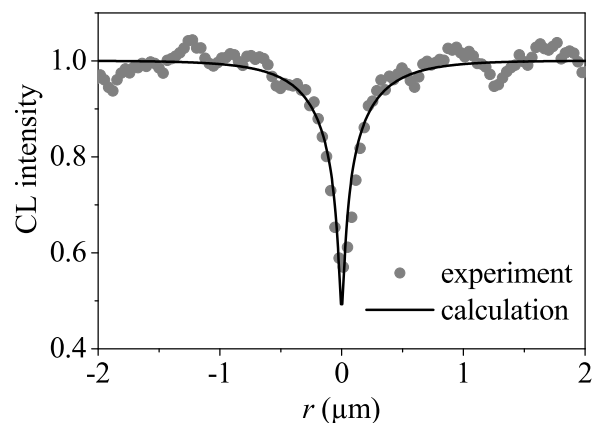


FIG. 7. Experimental CL intensity profile across a threading dislocation in our free-standing GaN layer (symbols) together with a calculated profile (line) obtained by integrating over the simulated exciton distribution generated by the electron beam with an acceleration voltage of 3 keV, with an exciton diffusion length of  $\Lambda = 0.4 \mu\text{m}$ , a surface recombination length of  $l_1 = 0.5 \mu\text{m}$ , a dislocation radius  $R = 1 \text{ nm}$ , and a dislocation recombination length of  $l_2 = 275 \mu\text{m}$ .

$D = 1.7 \text{ cm}^2/\text{s}$ ,  $S = 5 \times 10^4 \text{ cm/s}$ , and  $\tau \approx 1 \text{ ns}$ , which gives  $\Lambda = \sqrt{D\tau} = 0.4 \text{ }\mu\text{m}$  and  $l_1 = S\tau = 0.5 \text{ }\mu\text{m}$ .

We fit the experimental curve in Fig. 7 taking the surface recombination length fixed at  $l_1 = 0.5 \text{ }\mu\text{m}$  and obtain a diffusion length  $\Lambda = 0.4 \text{ }\mu\text{m}$ , in an excellent agreement with the results of Ref. [39], and the recombination length at the dislocation  $l_2 = 275 \text{ }\mu\text{m}$ . When we fix the surface recombination length  $l_1$  at values either larger or smaller by an order of magnitude, we obtain fits practically coinciding with the one shown in Fig. 7. The values of the exciton diffusion length and the dislocation recombination length are found to be  $\Lambda = 0.52 \text{ }\mu\text{m}$  and  $l_2 = 356 \text{ }\mu\text{m}$  in the former and  $\Lambda = 0.35 \text{ }\mu\text{m}$  and  $l_2 = 148 \text{ }\mu\text{m}$  in the latter case, respectively. These values provide an estimate of the accuracy in determination of the parameters in the case when the surface recombination length is not known.

## VI. SUMMARY AND CONCLUSIONS

We have presented a rigorous, complete, and general solution for the problem of excitons with an arbitrary initial distribution recombining in the bulk as well as diffusing toward a planar (the surface) and a linear (the dislocation) defect both being characterized by arbitrary, finite recombination velocities. This solution gives access, in principle, to three technologically important quantities: the surface recombination velocity, the recombination strength at the dislocation, and the exciton diffusion length. Our calculations have shown, however, that the former of these quantities has only a minor impact as long as the CL intensity cannot be measured on an

absolute scale. As a result, normalized intensity profiles allow one to uniquely extract both the recombination strength at the dislocation and the exciton diffusion length.

Regarding the former, our analysis shows that the threading dislocations in GaN(0001) layers are extremely efficient non-radiative centers, similar to those in other III-V compounds [40]. Concerning the latter, let us first stress that the diffusion length is not a material constant, as it seems to be often perceived, but a figure of merit for the purity and perfection of a given sample. More specifically, the diffusion length depends on the exciton diffusivity, and thus, via the Einstein relation, on its mobility, as well as on its lifetime. At room temperature, the exciton mobility should be limited by polar optical phonon scattering, and is thus expected to not vary significantly among samples with moderate defect densities. However, the exciton lifetime in GaN is still far from being determined by intrinsic radiative recombination, but is controlled by nonradiative, Shockley-Read-Hall type recombination at defect states [41]. The room temperature diffusion length in samples with very low dislocation density, as the one used in the present work, thus provides insight into the impact of point defects on the internal quantum efficiency of GaN.

## VII. ACKNOWLEDGMENTS

We are indebted to Uwe Jahn for a critical reading of the manuscript. K. K. S. kindly acknowledges the support of Russian Science Foundation under grant N 14-11-00083.

- 
- <sup>1</sup> S. D. Lester, F. A. Ponce, M. G. Craford, and D. A. Steigerwald, "High dislocation densities in high efficiency GaN-based light-emitting diodes," *Appl. Phys. Lett.* **66**, 1249 (1995).
  - <sup>2</sup> S. J. Rosner, E. C. Carr, M. J. Ludowise, G. Girolami, and H. I. Erikson, "Correlation of cathodoluminescence inhomogeneity with microstructural defects in epitaxial GaN grown by metalorganic chemical-vapor deposition," *Appl. Phys. Lett.* **70**, 420 (1997).
  - <sup>3</sup> T. Sugahara, H. Sato, M. Hao, Y. Naoi, S. Kurai, S. Tottori, K. Yamashita, K. Nishino, L. T. Romano, and S. Sakai, "Direct evidence that dislocations are non-radiative recombination centers in GaN," *Jpn. J. Appl. Phys.* **37**, L398 (1998).
  - <sup>4</sup> Z. Z. Bandić, P. M. Bridger, E. C. Piquette, and T. C. McGill, "The values of minority carrier diffusion lengths and lifetimes in GaN and their implications for bipolar devices," *Solid State Electron.* **44**, 221 (2000).
  - <sup>5</sup> L. Chernyak, A. Osinsky, and A. Schulte, "Minority carrier transport in GaN and related materials," *Solid State Electron.* **45**, 1687 (2001).
  - <sup>6</sup> S. Yu. Karpov and Yu. N. Makarov, "Dislocation effect on light emission efficiency in gallium nitride," *Appl. Phys. Lett.* **81**, 4721 (2002).
  - <sup>7</sup> C. Donolato, "Contrast and resolution of SEM charge-collection images of dislocations," *Appl. Phys. Lett.* **34**, 80 (1979).
  - <sup>8</sup> J. R. Haynes and W. Shockley, "The mobility and life of injected holes and electrons in germanium," *Phys. Rev.* **81**, 835 (1951).
  - <sup>9</sup> S. Visvanathan and J. F. Battey, "Some problems in the diffusion of minority carriers in a semiconductor," *J. Appl. Phys.* **25**, 99 (1954).
  - <sup>10</sup> J. P. McKelvey and R. L. Longini, "Recombination of injected carriers at dislocation edges in semiconductors," *Phys. Rev.* **99**, 1227 (1955).
  - <sup>11</sup> W. Van Roosbroeck, "Injected current carrier transport in a semi-infinite semiconductor and the determination of lifetimes and surface recombination velocities," *J. Appl. Phys.* **26**, 380 (1955).
  - <sup>12</sup> C. Donolato, "On the theory of SEM charge-collection imaging of localized defects in semiconductors," *Optik* **52**, 19 (1978).
  - <sup>13</sup> A. Jakubowicz, "On the theory of electron-beam-induced current contrast from pointlike defects in semiconductors," *J. Appl. Phys.* **57**, 1194 (1985).
  - <sup>14</sup> C. Donolato, "A reciprocity theorem for charge collection," *Appl. Phys. Lett.* **46**, 270 (1985).
  - <sup>15</sup> A. Jakubowicz, "Theory of cathodoluminescence contrast from localized defects in semiconductors," *J. Appl. Phys.* **59**, 2205 (1986).
  - <sup>16</sup> C. Donolato, "A theoretical study of the charge collection contrast of localized semiconductor defects with arbitrary recombination activity," *Semicond. Sci. Technol.* **7**, 37 (1992).
  - <sup>17</sup> C. Donolato, "Modeling the effect of dislocations on the minority carrier diffusion length of a semiconductor," *J. Appl. Phys.* **84**, 2656 (1998).
  - <sup>18</sup> T. Suzuki and Y. Matsumoto, "Effects of dislocations on photoluminescent properties in liquid phase epitaxial GaP," *Appl. Phys.*

- Lett. **26**, 431 (1975).
- 19 D. Cherns, S. J. Henley, and F. A. Ponce, "Edge and screw dislocations as nonradiative centers in InGaN/GaN quantum well luminescence," *Appl. Phys. Lett.* **78**, 2691 (2001).
  - 20 D. Nakaji, V. Grillo, N. Yamamoto, and T. Mukai, "Contrast analysis of dislocation images in TEM–cathodoluminescence technique," *J. Electron Microscopy* **54**, 223 (2005).
  - 21 N. Pauc, M. R. Phillips, V. Aimez, and D. Drouin, "Carrier recombination near threading dislocations in GaN epilayers by low voltage cathodoluminescence," *Appl. Phys. Lett.* **89**, 161905 (2006).
  - 22 N. Ino and N. Yamamoto, "Low temperature diffusion length of excitons in gallium nitride measured by cathodoluminescence technique," *Appl. Phys. Lett.* **93**, 232103 (2008).
  - 23 N. Pauc, M. R. Phillips, V. Aimez, and D. Drouin, "Response to "Comment on 'Carrier recombination near threading dislocations in GaN epilayers by low voltage cathodoluminescence'" [Appl. Phys. Lett. 97, 166101, 2010]," *Appl. Phys. Lett.* **97**, 166102 (2010).
  - 24 E. B. Yakimov, "Comment on "Carrier recombination near threading dislocations in GaN epilayers by low voltage cathodoluminescence" [Appl. Phys. Lett. 89, 161905, 2006]," *Appl. Phys. Lett.* **97**, 166101 (2010).
  - 25 E. B. Yakimov, "What is the real value of diffusion length in GaN?" *J. Alloys Compounds* **627**, 344 (2015).
  - 26 Th. Kieliba, S. Riepe, and W. Warta, "Effect of dislocations on minority carrier diffusion length in practical silicon solar cells," *J. Appl. Phys.* **100**, 063706 (2006).
  - 27 V. Budhraj, B. Sopori, N. Ravindra, and D. Misra, "Improved dislocation model of silicon solar cells with the effect of front and back surface recombination velocity," *Prog. Photovolt.: Res. Appl.* **22**, 1256 (2014).
  - 28 W. A. Brantley, O. G. Lorimor, P. D. Dapkus, S. E. Haszko, and R. H. Saul, "Effect of dislocations on green electroluminescence efficiency in GaP grown by liquid phase epitaxy," *J. Appl. Phys.* **46**, 2629 (1975).
  - 29 M. Lax, "Junction current and luminescence near a dislocation or a surface," *J. Appl. Phys.* **49**, 2796 (1978).
  - 30 M. Toth and M. R. Phillips, "Monte Carlo modeling of cathodoluminescence generation using electron energy loss curves," *Scanning* **20**, 425 (1998).
  - 31 H. Demers, N. Poirier-Demers, A. R. Couture, D. Joly, M. Guilman, N. de Jonge, and D. Drouin, "Three-dimensional electron microscopy simulation with the CASINO Monte Carlo software," *Scanning* **33**, 135 (2011).
  - 32 H. Demers, N. Poirier-Demers, M. R. Phillips, N. de Jonge, and D. Drouin, "Three-dimensional electron energy deposition modeling of cathodoluminescence emission near threading dislocations in GaN and electron-beam lithography exposure parameters for a PMMA resist," *Microsc. Microanal.* **18**, 1220 (2012).
  - 33 C. Donolato, "An analytical model of SEM and STEM charge collection images of dislocations in thin semiconductor layers," *Phys. Stat. Sol. (a)* **65**, 649 (1981).
  - 34 C. Donolato, "On the analysis of diffusion length measurements by SEM," *Solid State Electron.* **25**, 1077 (1982).
  - 35 U. Werner, F. Koch, and G. Oelgart, "Kilovolt electron energy loss distribution in Si," *J. Phys. D: Appl. Phys.* **21**, 116 (1988).
  - 36 C. M. Parish and P. E. Russell, "On the use of Monte Carlo modeling in the mathematical analysis of scanning electron microscopy–electron beam induced current data," *Appl. Phys. Lett.* **89**, 192108 (2006).
  - 37 E. B. Yakimov, S. S. Borisov, and S. I. Zaitsev, "EBIC measurements of small diffusion length in semiconductor structures," *Semiconductors* **41**, 411 (2007).
  - 38 N. M. Shmidt, O. A. Soltanovich, A. S. Usikov, E. B. Yakimov, and E. E. Zavarin, "High-resolution electron-beam-induced-current study of the defect structure in GaN epilayers," *J. Phys.: Condens. Matter* **14**, 13285 (2002).
  - 39 R. Aleksiejūnas, M. Sūdžius, T. Malinauskas, J. Vaitkus, K. Jarašiūnas, and S. Sakai, "Determination of free carrier bipolar diffusion coefficient and surface recombination velocity of undoped GaN epilayers," *Appl. Phys. Lett.* **83**, 1157 (2003).
  - 40 S. Hildebrandt, J. Schreiber, W. Hergert, H. Uniewski, and H. S. Leipner, "Theoretical fundamentals and experimental materials and defect structures using quantitative scanning electron microscopy-cathodoluminescence/electron beam induced current on compound semiconductors," *Scanning Microscopy* **12**, 535 (1998).
  - 41 P. Ščajev, K. Jarašiūnas, S. Okur, Ü. Özgür, and H. Morkoç, "Carrier dynamics in bulk GaN," *J. Appl. Phys.* **111**, 023702 (2012).